Anuário do Instituto de Geociências - UFRJ
www.anuario.igeo.ufrj.br

Ocean-Atmosphere Interactions in an Extratropical Cyclone in the Southwest Atlantic

Interações Oceano-Atmosfera em um Ciclone Extratropical no Atlântico Sudoeste

Ueslei Adriano Sutil[1]; Luciano Ponzi Pezzi[1];
Rita de Cássia Marques Alves[2] & André Becker Nunes[3]

[1]National Institute for Space Research, Earth Observation General Coordination,
Avenida dos Astronautas, 1.758, 12227-010, Jardim da Granja, São José dos Campos, SP, Brazil
[2]Federal University of Rio Grande do Sul, State Center for Remote Sensing and Meteorology Research,
Avenida Bento Gonçalves, 9500, 91501-970, Campus do Vale, Porto Alegre, RS, Brazil
[3]Center for Research and Meteorological Forecast, Federal University of Pelotas
Rua Gomes Carneiro, 1, 96010-610, Centro, Pelotas, RS, Brazil
E-mails: uesleisutil1@gmail.com; luciano@dsr.inpe.br; rita.cma@terra.com.br; beckernunes@gmail.com
Recebido em: 05/10/2018 Aprovado em: 08/02/2019
DOI: http://dx.doi.org/10.11137/2019_1_525_535

Abstract

This work shows an investigation of the behavior of heat fluxes in the processes of ocean-atmosphere interaction during the passage of an Extra-tropical Cyclone (EC) in the Southwest Atlantic in September 2006 using a coupled regional model's system. A brief evaluation of the simulated data is done by comparison with air and sea surface temperature (SST) data, wind speed, sea level pressure. This comparison showed that both model simulations present some differences (mainly, the wind), nevertheless the simulated variables show quite satisfactory results, therefore allowing a good analysis of the ocean-atmosphere interaction processes. The simulated thermal gradient increases the ocean's heat fluxes into the atmosphere in the cold sector of the cyclone and through the convergence of low level winds the humidity is transported to higher levels producing precipitation. The coupled system showed a greater ability to simulate the intensity and trajectory of the cyclone, compared to the simulation of the atmospheric model.
Keywords: ocean-atmosphere interaction, oceanography, meteorology.

Resumo

Este trabalho apresenta uma investigação do comportamento dos fluxos de calor nos processos de interação oceano-atmosfera durante a passagem de um ciclone extra tropical (EC) no Atlântico sudoeste em setembro de 2006 usando um sistema de modelos regionais acoplados. Uma breve avaliação dos dados simulados é feita em comparação com os dados da Temperatura do Ar e da Superfície do Mar (SST), Velocidade do Vento, Pressão ao Nível Médio do Mar. Esta comparação mostrou que ambas as simulações de modelos apresentam algumas diferenças (principalmente, o vento), no entanto, as variáveis simuladas mostram resultados bastante satisfatórios, permitindo assim uma boa análise dos processos de interação oceano-atmosfera. O gradiente térmico simulado aumenta os fluxos de calor do oceano para a atmosfera no setor frio do ciclone e, através da convergência de ventos de baixo nível, a umidade é transportada para níveis mais altos produzindo precipitação. O sistema acoplado mostrou uma maior habilidade para simular a intensidade e trajetória do ciclone, em comparação com a simulação do modelo atmosférico.
Palavras-chave: interação oceano-atmosfera, oceanografia, meteorologia.

1 Introduction

The Southwest Atlantic Ocean (SWA) circulation is well described in the works, Sverdrup *et al*. (1942) and Emílson (1959; 1961). This region is characterized by the complex water masses and currents variability, as studied also by Stramma & England (1999), and more recently, by Pezzi *et al*. (2016a) review work.

Souza & Robinson (2003) mention that surface oceanic dynamics of the region is defined by the Brazilian Counter Current (BCC), which is limited in extent by the action of the winds and by the flow of the La Plata River and flows northeastward within the Continental Shelf (CS). The northern region is bordered by the Brazil Current (BC), which flows to the southeast along the CS break, originating from the bifurcation of the Equatorial South Current in 10 °S. BC is defined as a warm current of the western boundary of the South Atlantic Subtropical Gyre (Garzoli & Matano, 2011; Campos, 2014). The Malvinas Current (MC) is derived from the Antarctic Circumpolar Current and is described as a cold current flowing northwest, being less saline than CB. At approximately 35 °S, the CM and the CB form the Brazil-Malvinas Confluence (BMC). Lentini *et al*. (2002), Pezzi *et al*. (2005, 2009, 2016b), Pezzi & Souza (2009), Souza *et al*. (2006) and Mendonça *et al*. (2017) says that CBM has strong temperature and saline gradients. Because of its complex dynamics, the region is commonly described as one of the most complex and energetic in the ocean world (Souza & Robinson, 2003; Chelton *et al*., 2004).

The meteorological conditions in southern Brazil are affected mainly by frontal systems, mesoscale convective systems, cyclonic systems at medium levels of the atmosphere, upper levels cyclonic vortices and cyclones (Cavalcanti *et al*., 2009), and according to the study of Hoskins & Hodges (2005), this region is also a cyclogenetic area where Extratropical Cyclones (EC) are formed.

These EC can represent a threat to the southeast of South America and generate serious damages to the impacted regions, as observed in Parise *et al*. (2009), whose comment about the erosion on the southern Brazilian coast caused by an EC. Despite this risk, there's a lack in ocean-atmosphere studies in Brazil, according to Pezzi *et al*. (2016a), mainly related by the difficulty of obtaining oceanographic and atmospheric *in situ* data, despite the effort to monitor remotely the ocean and atmosphere through satellite derived data (Campos, 2014)

In order to address this problem, the ocean--atmosphere numerical modeling system can be an important tool to study the air-sea interaction due to its efficiency of representing the terrestrial system, as studied by Chelton (2004), Xie (2004), Seo *et al*. (2006), Miller *et al*. (2017) and Mendonça *et al*. (2017). It is also a promising tool in the study of ECs, as noted by Pullen *et al*. (2018), which compared a simulation of the hybrid hurricane *Catarina* (Mctaggart-Cowan *et al*., 2006) using a coupled ocean-atmosphere modeling system and a simulation using only an atmospheric model that landed in the Brazilian south coast in 2004. It was shown in this study (Pullen *et al*., 2018) that the coupled model simulated a better trajectory to *Catarina* when compared to the simulation in which only the atmospheric model is used. This fact is also presented in our work.

Based on the above exposed, the main objective of this work is to investigate the effects of the ocean-atmosphere coupling on the simulations of a strong EC that reached the southern region of Brazil in September 2006. According to Parise *et al*. (2009), this EC generated an intense storm surge at southern Brazilian coast, with an intense horizontal tide displacement. Here it was used a set of numerical experiments were performed using two way coupled ocean and atmosphere models and another using only atmospheric model with the prescribed Sea Surface Temperature (SST).

2 Methods

2.1 COAWST

In this study the Coupled-Ocean-Atmosphere--Wave-Sediment Transport v 3.2 (COAWST) (Warner *et al*., 2010), was used. The COAWST combines four well-known models, allowing an active coupling between the ocean and the atmosphere. The Weather Research and Forecasting Model v3.7.1 (WRF) (Skamarock *et al*., 2005) is the atmospheric

Anuário do Instituto de Geociências - UFRJ
ISSN 0101-9759 e-ISSN 1982-3908 - Vol. 42 - 1 / 2019 p. 525_535

model, the Regional Ocean Modeling System svn 797 (ROMS) (Shchepetkin & Mcwilliams, 2005; Haidvogel *et al*., 2008) is the hydrodynamic model, the Simulating Waves Nearshore v 41.01AB (SWAN) (Booij *et al*., 1999) is the wave model and the Community Sediment Transport Modeling Systems (CSTM) (Warner *et al*., 2008) is the sediment transport model. For this study, the SWAN and the CSTM were not activated. All these models are fully coupled using the Model Coupling Toolkit v 2.6.0 (MCT) (Larson *et al*., 2005) and since ROMS and WRF have different grids, the weights between each model grid are interpolated using the Spherical Coordinate Remapping Interpolation Package (SCRIP) (Jones, 1999). The exchanges between the models are represented in the Figure 1.

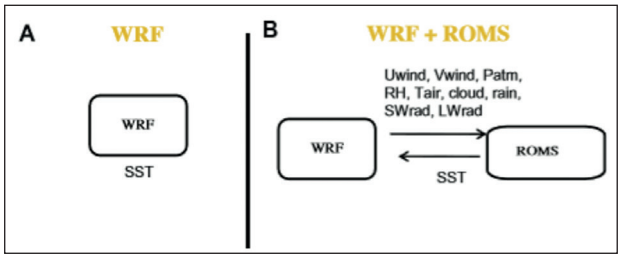

Figure 1 COAWST configurations used in this study involving the WRF model A. WRF only; and B. WRF-ROMS coupling (Adapted from Figure 5 of Warner *et al*., 2010).

2.2 WRF Configuration

The WRF solves a set of fully non-compressible, non-hydrostatic and Eulerian equations in terrain-following coordinates, with a variety of physical parameterizations of sub-grid scale processes. The model predicts three-dimensional components of wind, surface pressure, dew point, precipitation, latent and sensitive heat fluxes, long and shortwave radiation fluxes, relative humidity and air temperature in grids with eta vertical coordinates (Skamarock *et al*., 2008).

The WRF domain extends between 5°S to 50°S and 70°W and 20°W, with 20 seconds time-step. The horizontal resolution is 6 km with 44 vertical levels from sea level up to 50 mb. The initial and boundary conditions were obtained from the NCEP Climate Forecast System reanalysis (CFSR), which has 0.5° x 0.5° of spatial resolution and 6 hours of temporal resolution.

The choices of physical parameterizations used were based in previous studies found in the literature (Shi *et al*., 2010; Tao *et al*., 2011; Nicholls & Decker, 2015):

- Longwave radiation: new Goddard scheme (Chou & Suarez, 1999; Shi *et al*., 2010);
- Shortwave radiation: new Goddard scheme (Chou & Suarez, 1999);
- Surface layer: Eta similarity (Monin & Obukhov, 1954; Janjic, 2002);
- Land surface: Unified Noah Land Surface Model (Chen & Dudhia, 2001);
- Boundary layer: Mellor-Yamada-Janjic (Mellor & Yamada, 1982; Janjic, 2002);
- Cumulus parameterization: Kain-Fritsch (Kain, 2004);
- Microphysics: Goddard Scheme (Lang *et al*., 2007).

2.3 ROMS Configuration

ROMS is an oceanic tridimensional regional model with free-surface and terrain-following in sigma coordinates. The model integrates the Navier-Stokes equations into Reynolds 3D averages, using hydrostatic approximations. ROMS uses finite difference approximations on an Arakawa-C curvilinear horizontal grid. Momentum, scalar advection and diffusive processes are solved using transport equations, and an equation of state computes the density field. ROMS provides a flexible structure that allows multiple choices for many model components, such as options for advection numerical schemes, turbulence, boundary conditions, sub-layers for surface and bottom layers, air-sea flows among other features (Shchepetkin & Mcwilliams, 2005; Haidvogel *et al*., 2008).

The ROMS domain is identical the one used for WRF grid, however with finer horizontal resolution. ROMS was configured with 1/12° horizontal resolution and 30 sigma levels of depth, with 40 s barotropic and 90 s baroclinic time-steps. The surface and bottom stretching parameter are 5 and 0.6, respectively, with a 50 m critical depth controlling the stretching and default vertical coordinate trans-

formation. The main physical parameterizations options activated for this study are:

- Momentum equations: Horizontal harmonic viscosity of momentum (Waksowicz, 1993);
- Tracers equations: 3rd-order upstream horizontal advection and 4th-order centered horizontal advection (S*hchepetkin & Mcwilliams,* 2005)
- Pressure gradient algorithm: Spline Jacobian density (S*hchepetkin & Mcwilliams,* 2003);
- Wave roughness formulation: Taylor and Yelland relation (Taylor & Yelland, 2001);
- Horizontal mixing of momentum: Constant S-surfaces *(Shchepetkin & Mcwilliams,* 2003);
- Horizontal mixing of tracers: Geopotential (constant depth) surfaces (S*hchepetkin & Mcwilliams,* 2003);
- Vertical mixing of momentum and tracers: Generic Lenght-Scale (Warner *et al*., 2004).

The initial and boundary conditions were obtained from Simple Ocean Data Assimilation (SODA) (Carton & Giese, 2008), which has 0.5° x 0.5º spatial resolution and temporal resolution every 5 days.

2.4 Experimental Design and Auxiliary Data

Two numerical experiments were performed. They started on August 19th 2006 and finished on September 8th 2006. The first experiment used only atmospheric model (named WRF_EXP) and the second one coupling WRF and the hydrodynamic model ROMS (named COA_EXP), as show in Figure 2a and 2b, respectively. In the coupled simulation, the WRF model provides to ROMS fields of U and V wind components, atmospheric pressure, relative humidity, air temperature, clouds, precipitation, longwave radiation and shortwave radiation. In turn ROMS will provide Sea Surface Temperature (SST) to WRF. The frequency of fields exchanges between WRF and ROMS is at every 1800 seconds, with both simulations being saved every 6 hours. Also, following the work of Mooney *et al*. (2016), we performed a short 10 days spin-up period for both simulations.

In order to compare the simulated precipitation with independent data, we used the Climate Prediction Center Morphing Technique (CMORPH) from the National Ocean and Atmosphere Administration (NOAA) that is described in Joyce *et al*. (2004). This dataset is estimated by algorithms based on Ferraro (1997), Ferraro *et al*. (2000) and Kummerow *et al*. (2001), and has spatial resolution of 0.25º × 0.25º and temporal resolution of 30 minutes. Also, we used *in situ* data from three Brazilian meteorological stations located in the cities of Rio Grande (32º 03'S and 52º 11'W), Torres (29º 21'S and 49º 43'W), and Florianópolis (27º 36'S and 48º 36'W) from the National Institute of Meteorology (INMET). The variables used were the wind at 10 meters, the mean sea level pressure and the air temperature at 2 meters available every 06 hours from 27th August 2006 to 8th September, 2006.

3 Results

3.1 Model Evaluations

The oceanic COA_EXP results (ROMS derived) are evaluated by comparing its simulated SST with the prescribed SST used in WRF_EXP simulation. It is important to remark that this is CFSR SST, as shown in Figure 2a and 2b. The simulated SST by COA_EXP (Figure 2A) satisfactorily reproduces the major oceanic features that are also seen in WRF_EXP. However, it is important to note that COA_EXP results have many mesoscale features and phenomena that are explicitly solved due to higher resolution of the oceanic model compared to that SST used in WRF_EXP experiment, where these features are smoothened or not represented. This is a clear case where the model horizontal resolution is playing a role. An example can be seen in the BCC at the Southern Brazilian Continental Shelf (SBCS), which is well represented in COA_EXP and quite smoothened in WRF_EXP. The role of this thermal front in the MABL stability modulation was explored in Pezzi *et al*. (2016b). On the other hand, analyzing the differences we can see two distinct sectors (Figure 2c). Between 33°S and 50°S, the SST of COA_EXP is up to 5ºC higher than WRF_EXP, while in remain of the domain the simulated SST is up to 3.5ºC lower than WRF_EXP. The root mean square

Anuário do Instituto de Geociências - UFRJ
ISSN 0101-9759 e-ISSN 1982-3908 - Vol. 42 - 1 / 2019 p. 525_535

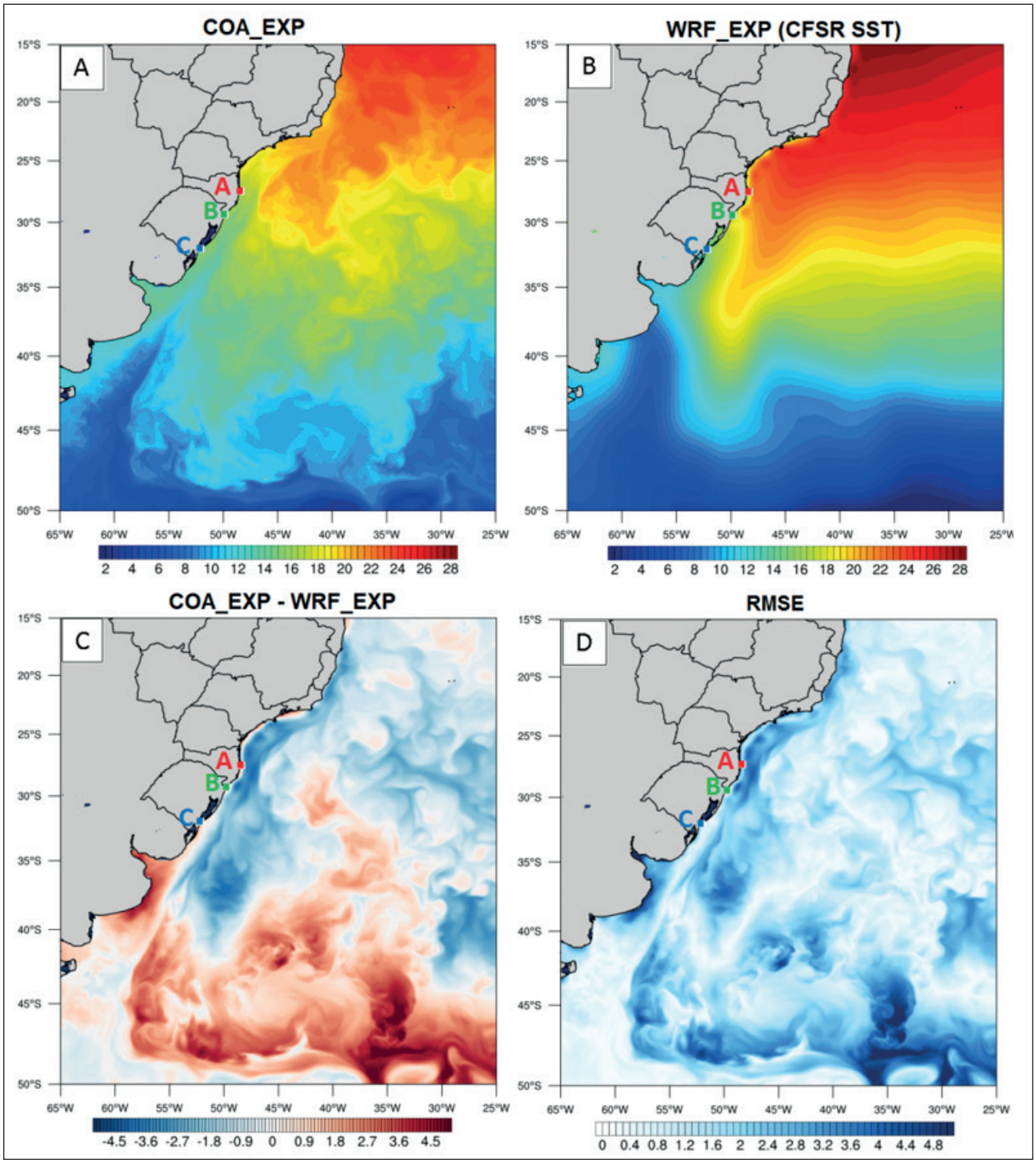

Figure 2 A. SST (ºC) simulated by COA_EXP; B. SST (ºC) from CFSR used in WRF; C. difference between SST (ºC) simulated by COA_EXP and D. CFSR SST used in WRF_EXP RSME between COA_EXP from SST (°C) and CFSR.

error (RMSE) (Wilks, 1995) was used to measure the differences between the simulated values and the observed data used as control. The errors found (Figure 2d) are up to 5 °C between 50°S and 45°S and 37°W and 29°W, while in other regions the simulation presented errors ranging from 0 to 4.43 °C.

The Taylor Diagram (Taylor, 2001) was used to evaluate the simulated data by COA_EXP and WRF_EXP relative to the three meteorological stations. For that, wind magnitude at 10 meters (W10), sea level pressure (SLP) and air temperature at 2 meters (Tair) were used. COA_EXP simulation showed a correlation between 0.8 and 0.97 and standard deviation between 0.25 and 0.78 for the Tair and SLP data, while the data simulated by the WRF_EXP showed correlation between 0.73 and 0.96 and standard deviation between 0.25 and 0.78. V_{10} presented a correlation of 0.1 and 0.47 and a standard deviation between 0.77 and 1.33 in the simulation with COA_EXP, whereas the COA_EXP data showed a correlation between 0.1 and 0.3 and a standard deviation between 1.22 and 1.31 (Figure 3). Santos-Alamillos *et al*. (2013) suggested that discrepancies found in simulations with WRF may be sensitive both to the terrain topography and to the horizontal resolution used.

Our comparative analysis shown in Figures 2 and 3 reveals that both simulations present some errors and differences when compared to observations, mainly in the near surface wind. However, it is also noticed that the simulations of COA_EXP and WRF_EXP produce very reasonable simulations when analyzing SLP and Tar during the EC passage. This first analysis of comparison of the simulations with the observed data, assured the quality of our simulations giving confidence to proceed an analysis with more details about the air-sea interaction processes that occurred during the passage of the EC chosen for this case study.

3.2 Extratropical Cyclone Analysis

The EC trajectory is shown in Figure 4. The minimum SLP points of the two simulations and the CFSR data were extracted at every 6 hours, from September 2nd at 00:00 UTC to September 5th at 00:00 UTC. It's observed that the coupling between the oceanic and atmospheric models provides a better simulation of the EC path when compared to the WRF simulation. The COA_EXP simulates the trajectory closer to the CFSR. Although both simulations present some differences in the cyclone positions when compared with the CFSR data. At September 4 at 00:00 UTC the EC simulated by the WRF model moves northeast, not following the route provided by the CFSR. The result is similar to that found in Pullen *et al*. (2018), which demonstrated that the active coupling between ocean and atmospheric models provides more accurate results.

The LHF, wind direction and speed at 10 meters simulated by COA_EXP and WRF_EXP for September 3rd at 12:00 UTC, are presented in Figure

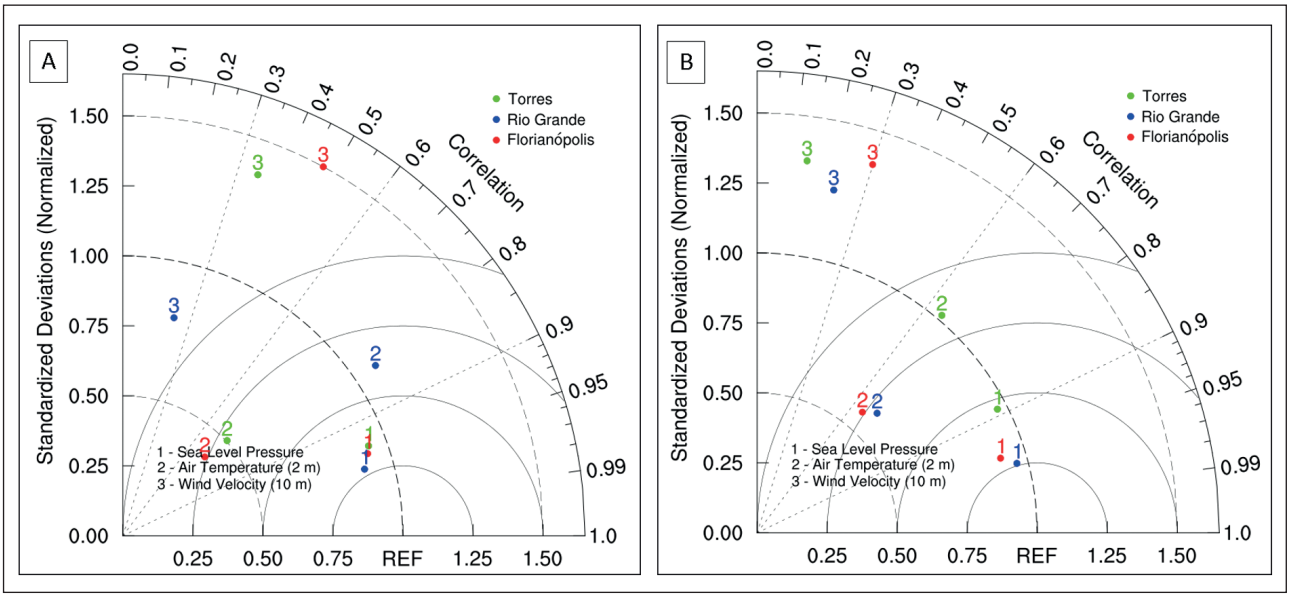

Figure 3 Taylor diagrams comparing the mean sea level pressure, air temperature and wind velocity of the simulation generated with the meteorological stations of Torres (green), Rio Grande (blue) and Florianópolis (Red); A. COA_EXP; and B. WRF_EXP.

Anuário do Instituto de Geociências - UFRJ
ISSN 0101-9759 e-ISSN 1982-3908 - Vol. 42 - 1 / 2019 p. 525_535

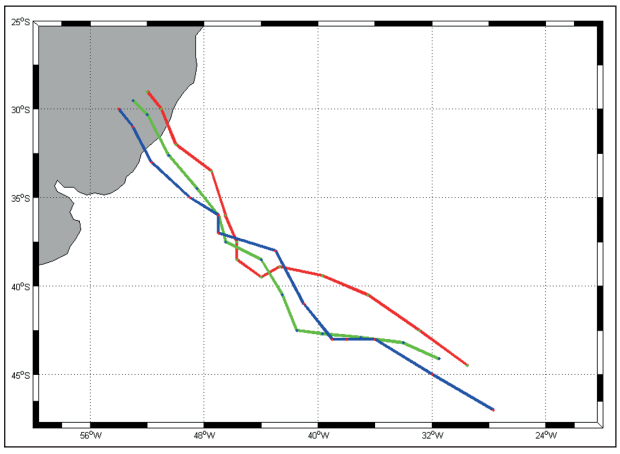

Figure 4 Extratropical cyclone trajectory extracted using minimum SLP data from COA_EXP (green line), WRF_EXP (red line) and CFSR (blue line) reanalysis.

5, day in which the EC central pressure was lower and LHF had the maximum value. In general, the COA_EXP fluxes were more realistic than the fluxes simulated by WRF_EXP, when compared to the CFSR. Larger LHF values were found due to the intensification of surface winds as a consequence of the horizontal pressure gradient, For the WRF_EXP, LHF fluxes exceeded 550 W m^{-2}, COA_EXP exceeded 500 W m^{-2} while CFSR 600 W m^{-2} over point near the southern region of Brazil and Uruguay. But both simulations showed an extensive region with LHF between 400 W m^{-2} and 500 W m^{-2}.

The differences between the simulations are due to the exchange between the oceanic and atmospheric models in the COA_EXP, which provides more accurate information for the LHF, mainly in the pattern that the LHF is distributed in the cold sector of the EC between 45ºS to 38ºS and 56ºW to 48ºW in COA_EXP, which has a shape more similar to the CFSR than the WRF_EXP. In Figure 2a and 2b it is observed that SST values of the COA_EXP are larger than the SST in the WRF_EXP dataset for that region, having a key role in the behavior of the LHF. This fact and demonstrates that coupled regional modeling is a promising tool to the simulation of the LHF in this region. Despite this, when compared to CFSR, COA_EXP underestimates the LHF values up to 170 W m^2 at 30ºS and 35ºS and 51ºW to 46ºW, possibly associated to the initial condition used in COA_EXP that presented lower SST values when compared with WRF_EXP. LHF transfer to the atmosphere occurs over the warm waters of the BC during this EC event. This behavior is similar to what has been demonstrated by Pezzi *et al*. (2005, 2009, 2016).

A north-south cross section at 45ºW for September 03rd at 12:00 UTC (Figure 6) was made, to understand the relationship between the convergence on the low level winds, LHF and precipitation. Near 39ºS there is a strong surface winds convergence in the central zone of the EC that causes upward

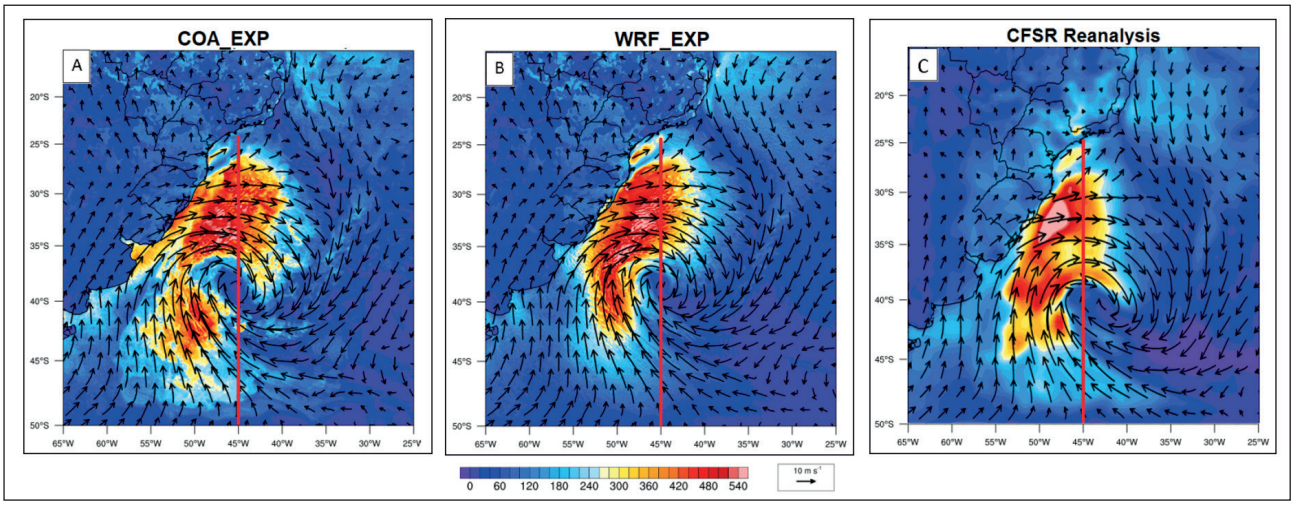

Figure 5 Latent Heat Flux (W m^{-2}, shaded) and Wind Speed and Direction in 10 m (m s^{-1}, vectors) for September 03rd, 2006 at 1200 UTC. The section in red represents the longitudinal section at 45ºW shown in Figure 6. (A) COA_EXP (B) WRF_EXP (C) and CFSR database.

motion in the atmosphere. Between 35ºS and 25ºS are the highest values of LHF, with mean values of 470 W m^{-2} in COA_EXP and 490 W m^{-2} in WRF. The weaker precipitation occurs in this area where are the cold and dry branch of the EC. In contrast, the opposite is observed at 45ºS to 37ºS where the higher precipitation rates are due to the warm branch of the EC, which produces maximum precipitations of 17 mm in the COA_EXP and 18.5 mm in the WRF. The same patterns are found in the simulations for the convergence of the winds and LHF when comparing with CFSR. Despite of it, LHF does not exceed 437 W m^{-2} in CFSR and the wind convergence in the EC center is weaker with maximum value of -2x10^{-4} s^{-1} while COA_EXP and WRF_EXP simulated their peaks of -6x10^{-4} s^{-1}. This difference can be associated with the lower spatial resolution of CFSR grid.

Another important result found is in the precipitation at 12:00 UTC. The CMORPH registers up to 3.8 mm in a region that has peaks of up to 2 mm of rainfall in both simulations, whereas in the region where the largest rainfall records occur, it does not register precipitation, characterizing the non-viability of using CMORPH data in the Analysis of this study.

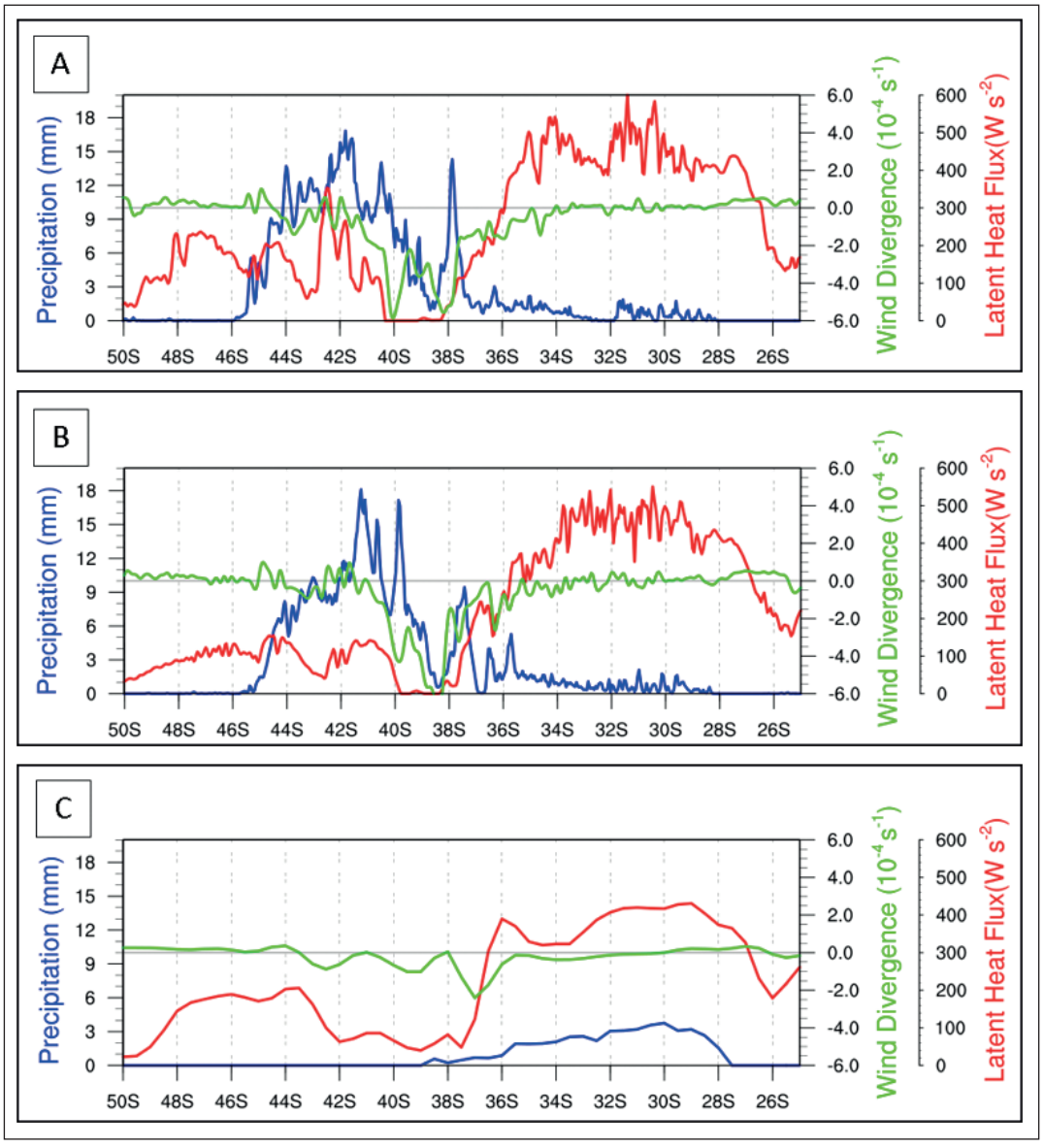

Figure 6 Meridional cut at 45°S for September 03, 2006 at 1200 UTC showing the Latent Heat Flux (Red line, W m^{-2}), Daily Precipitation (Blue line, mm) and Wind divergence in 10m (Green line, 10-4 s^{-1}). A. COA_EXP; B. WRF_EXP; C. the latent heat flux (red line, W m^{-2}) and the divergence of the winds in 10m (green line,10-4 s^{-1}) are from the CFSR and accumulated daily precipitation (blue line, mm) is from CMORPH.

Anuário do Instituto de Geociências - UFRJ
ISSN 0101-9759 e-ISSN 1982-3908 - Vol. 42 - 1 / 2019 p. 525_535

The analysis suggests that the ocean-atmosphere interaction destabilizes the atmosphere, changing the pattern of temperature, pressure, and wind fields. Initially, due to the passage of cold air in the surface, the ocean loses heat to the atmosphere, creating intense LHF gradients in both simulations. Latent heat is released to the atmosphere during the oceanic evaporation and the EC central pressure is decreased. Humidity in the lower atmosphere that converges to the center of the EC is upward transported. This thermodynamic process induces the precipitation caused by the EC. Similar result was described by Pezzi *et al*. (2016b), where they've made an transect through the strong thermal gradient that exists between CB and BCC and was mostly made in the absence of mesoscale atmospheric systems. However, at the end of this transect, a post-frontal atmospheric situation was sampled, in the presence of intense winds and cold thermal advection caused by an EC that had passed a few hours before. This caused the heat fluxes to be greatly increased, reaching values very close to those found here, by the regional models when they simulate the EC.

4 Conclusions

This work presented an air-sea interaction analysis when an EC occurred in the Southwest Atlantic between September 2nd and 5th, 2006, using the COAWST coupled modeling system (COA_EXP) and a simulation with an atmospheric model solo (WRF_EXP). Since *in situ* data in the Atlantic Southwest are very scarce, the coupled regional modeling appears as a promising way to supply crucial information and understanding of the oceanic and atmospheric phenomena, as discussed by Miller *et al*. (2017) and Pullen *et al*. (2018). We highlight the unprecedented of simulating an EC in the southwestern region of the South Atlantic, using regional coupled modeling with high spatial resolution (approximately 9.2 km). This technique allows the SST to be simulated with increased details using the coupled modeling system (COA_EXP), thus providing an active information exchange between the ocean and atmosphere. That is not the case while WRF uncoupled atmospheric model is employed, since it is passive to SST, i.e. it is not influenced by the atmospheric variables.

The coupled (COA_EXP) simulation presented differences when compared to the solo WRF (WRF_EXP). Evaluations of the simulated data showed an important difference in the wind field when compared to *in situ* data. However, as demonstrated by Santos-Alamillos *et al*. (2013), there may be variations in the wind field at 10 meters due to terrain topography sensitivity as well as the horizontal grid resolution used. It's important to remark that the simulated precipitation did not present a good comparison with CMORPH data in this study. In our results the simulated precipitation overestimated compared to CMORPH. This fact may be related to CMORPH precipitation estimation method of Ferraro (1997) and Ferraro *et al*. (2000) in contrast to the parameterizations used in the WRF. This was showed by Zhang *et al*. (2013) where they conclude that CMORPH tends to underestimate the precipitation magnitudes when compared with quality-controlled radar precipitation.

In general, both experiments well represent the LHF when compared to *in situ* data at very high frequency at CCB as seen Pezzi *et al*. (2016b) at CCB as shown in their Figure 8. They sampled the ocean and atmosphere across the thermal gradient between CB and CCB, and mostly of their measurements were made in the absence of mesoscale atmospheric systems. However, at the end of their transect, a post-frontal situation was sampled. They found intense winds and a cold thermal advection caused by an EC that had passed a few hours before their arrival at that area. This synoptic situation increased the air-sea fluxes that reach at values very close to those found here by the regional models when they simulate CE. The difference found in the FCL between regional models may also be related to the fact that the ocean is active in COA_EXP, which allows the representation of mesoscale ocean phenomena that are not present in the WRF_EXP. This is the case of ocean vortices seen in the COA_EXP simulation close to the CBM region and also in more pronounced thermal fronts, such as CB / CCB.

In this study, the importance of the Southwest Atlantic was evident for the region near the southern coast of Brazil and Uruguay, which influenced decisively the generation of FCL during the passage

and intensification of the cyclone. Most likely this is its role in most of the cyclogenesis occurring in this region. Thus, it is clear that much study still needs to be done on the mechanisms of surface heat flux generation, exchanges of it between ocean and atmosphere, as well as the parameterizations to be used in numerical models. In addition to this activity, it is suggested that more *in situ* observations and high temporal and spatial resolution be made to study these processes, as it was done in Pezzi *et al*. (2016a) and Mendonça *et al*. (2017) because this is a way to obtain more reliability in relation to the work that the physical parameterizations used in regional numerical models are doing.

5 Acknowledgments

The first author thank the funding support of CAPES Pro-Integration 55/2013. The authors have the following funded projects about Air-Sea Interaction in Atlantic and Austral Oceans: National Institute of Science and Technology of Cryosphere (CNPq/PROANTAR-704222/2009), Advanced Studies in Oceanography of Medium and High Latitudes (CAPES - 23038.004304/2014-28) and Brazilian Antartic Program (CNPQ 443013/2018-7). CNPq funds U. A. Sutil through fellowship of the Institutional Capacity Program (300684/2016-9) and L. P. Pezzi through the Research Productivity Program (CNPq 304009/2016-4). We thank Dr. John Warner and all colleagues who have worked on the COAWST modeling system development and the anonymous reviewers who helped raise the scientific quality of the article.

6 References

Booij, N.; Ris, R.C. & Holthuijsen, L.H. 1999. A third-generation wave model for coastal regions. Part I: Model description 05 validation. *Journal of Geophysical Research*, *104*(C4): 7649-7666.

Campos, E.J.D. 2014. O papel do oceano nas mudanças climáticas. *Revista USP*, *103*(12): 57-66.

Carton, J.A. & Giese, B.S. 2008. A reanalysis of ocean climate using Simple Ocean Data Assimilation (SODA). *Monthly Weather Review*, *136*: 2999-3017.

Cavalcanti, F.A.; Ferreira, N.J.; Dias, M.A.F & Justi, M.G.A. 2009. *Tempo e Clima no Brasil*. São Paulo, Oficina de Textos. 464 p.

Chelton, D.B. 2004. The Impact of SST Specification on ECMWF Surface Wind Stress Fields in the Eastern Tropical Pacific. *Journal of Climate*, *18*: 530-550.

Chen, S.S. & Dudhia, J. 2001. Coupling an advanced land surface-hydrology model with the Penn State-NCAR MM5 modeling system. Part I: Model description and implementation. *Monthly Weather Review*, *129*: 569-585.

Emílson, I. 1959. Alguns aspectos físicos e químicos das águas marinhas brasileiras. *Ciência e Cultura*, *11*(2): 44-54.

Emílson, I. 1961. The shelf and coastal waters off southern Brazil. *Boletim do Instituto Oceanográfico*, *11*(2): 101-112.

Ferraro, R.R. 1997. Special Sensor Microwave Imager Derived Global Rainfall Estimates for Climatological Applications. *Journal Geophysical Research*, *102*: 16715-16735.

Ferraro, R.R.; Weng, F.; Grody, N.C. & Zhao, L. 2000. Precipitation characteristics over land from the NOAA-15 AMSU Sensor. *Geophysical Research Letter*, *27*(17): 2669-2672.

Garzoli, S.L. & R.P Matano. 2011. The South Atlantic and the Atlantic Meridional Overturning Circulation. *Deep Sea Research part II: Tropical Studies in Oceanography*, *58*(17-18): 1837-1847.

Haidvogel, D.B.; Arango, H.G.; Budgell, W.P.; Cornuelle, B.D.; Curchitser, E; Di Lorenzo, E.; Fennel, K.; Geyer, W. R.; Hernann, A. J.; Lanerolle, L.; Levin, J.; McWilliams, J. C.; Miller, A. J.; Moore, A. M.; Powell, A. F.; Shchepetkin, C. R.; Signel, R. P.; Warner, J. C. & Wolkin, J. 2008. Regional ocean forecasting in terrain-following coordinates: model formulation and skill assessment. *Journal of Computational Physics*, *227*: 3595-3624.

Hoskins, B.J. & Hodges, K.I.A. 2005. New Perspective on Southern Hemisphere Storm Tracks, *Journal of Climate*, *18*: 4108-4129.

Janjic, Z.I. 2002. Nonsingular implementation of the Mellor-Yamada level 2.5 scheme in the NCEP meso model. *NCEP Office Note 437.* 61 p.

Jones, P. W. 1999. First and Second Order Conservative Remapping Schemes for Grids in Spherical Coordinates. *Monthly Weather Review*, *127*: 2204-2210.

Joyce, R.J.; Janowiak, J.E.; Arkin, P.A. & Xie, P. 2004. CMORPH: A method that produces global precipitation estimates from passive microwave and infrared data at high spatial and temporal resolution. *Journal of Hydrometeorology*, *05*: 487-503.

Kain, J.S. 2004. The Kain-Fritsch convective parameterization: an update. *Journal of Applied Meteorology*, *43*: 170-181.

Kummerow, C.H.; Olson, Y.; Yang, W.S.; Adler, S.; McCollum, R.F.; Ferraro, J.; Petty, R.; Petty, G.; Shin, D-B. & Wilheit, T.T. 2001. The evolution of the Goddard Profiling Algorithm (GPROF) for rainfall estimation from passive-microwave sensor. *Journal of Applied Meteorology*, *40*: 1801-1820.

Lang, S.; Tao, W.K.; Cifelli, R.; Olson, W.; Halverson, J.; Rutledge, S. & Simpson, J. 2007. Improving simulations of convective system from TRMM LBA: Easterly and westerly regimes. *Journal of the Atmospheric Sciences*, *64*: 1141-1164.

Larson, J.; Jacob, R. & Ong, E. 2005. The model coupling toolkit: A new Fortran90 toolkit for building multiphysics parallel coupled models. *International Journal of High Performance Computing Applications*, *19*: 277-292.

Lentini, C.A.D.; Olson, D.B. & Podestá, G. 2002. Statistics of Brazil Current rings observed from AVHRR: 1993 to 1998. *Geophysical Research Letters*, *29*(16): 58-1-58-4.

McTaggart-Cowan, R.; Bosart, L.F.; Davis, C. A.; Atallah, E.H.; Gyakum, J. R. & Emanuel, K. A. 2006. Analyses of hurricane Catarina. *Monthly Weather Review*, *134*: 3029-3053.

Mellor, G.L. & Yamada, T. 1982. Development of turbulence closure model for geophysical fluid problems. *Reviews*

of Geophysics and Space Physics, *20*: 851-875.

Mendonça, L.F.; Souza, R.B.; Aseff, C.R.C.; Pezzi, L.P.; Möller, O.O. & Alves, R.C.M. 2017. Regional modeling of the water masses and circulation annual variability at the Southern Brazilian Continental Shelf. *Journal of Geophysical Research: Oceans*, *122*(2): 1232-1253.

Monin, A.S. & Obukhov, A.M. 1954. Basic laws of turbulent mixing in the surface layer of the atmosphere. *Trudy Geofiz, Instituta Akademii Nauk, SSSR (Proceedings of Geophysics Institute, National Academy of Science, SSSR), 24*: 163-187.

Mooney, P. A.; Gill, D. O.; Mulligan F. J.; Bruyère, C. L. 2016. Hurricane simulation using different representations of atmosphere-ocean interaction: the case of Irene (2011). *Atmospheric Science Letters, 17*: 415-421.

Miller, A.J.; Collins, M.; Gualdi, S.; Jensen, T.G.; Misra, V.; Pezzi, L.P.; Pierce, D.W.; Putrasahan, D.; Seo, H. & Tseng, Y. 2017. Coupled ocean-atmosphere modeling and predictions. *Journal of Marine Research*, *75*: 361-402.

Nicholls, S.D. & Decker, S.G. 2015. Impact of coupling an Ocean Model to WRF Nor'easter Simulations. *Monthly Weather Review*, *143*: 4997-5016.

Parise, C.K.; Calliari, L.J. & Krushe, N. 2009. Extreme storm surges in the south of Brazil: atmospheric conditions and shore erosion. *Brazilian Journal of Oceanography*, *57*: 175-188.

Pezzi, L.P.; Souza, R.B.; Dourado, M.S.; Garcia, C.A.E.; Mata, M.M. & Silva-Dias, M.A.F. 2005. Ocean-atmosphere in situ observations at the Brazil-Malvinas Confluence Region. *Geophysical Research Letters*, *32*(22): L22603.

Pezzi, L.P. & Souza, R.B. 2009. Variabilidade de meso-escala e interação oceano-atmosfera no Atlântico Sudoeste. *In*: CAVALCANTI, F.A.; FERREIRA, N.J.; DIAS, M.A.F. & JUSTI, M.G.A. (Eds.). *Tempo e Clima no Brasil*. Oficina de Textos, p. 385-405.

Pezzi, L.P.; Souza, R.B.; Acevedo, O.; Wainer, I.; Mata, M.M.; Garcia, C.A.E. & Camargo, R. 2009. Multi-year measurements of the Oceanic and Atmospheric Boundary Layers at the Brazil-Malvinas Confluence Region. *Journal of Geophysical Research*, *114*: D19103.

Pezzi, L.P.; Souza, R.B. & Quadros, M.F.L. 2016a. Uma revisão dos Processos de Interação Oceano-Atmosfera em Regiões de Intenso Gradiente Termal do Oceano Atlântico Sul Baseada em Dados Observacionais. *Revista Brasileira de Meteorologia*, *31*: 428-453.

Pezzi, L.P.; Souza, R.B.; Farias, P.C. & Acevedo, O. 2016b. Air-sea interaction at the Southern Brazilian Continental Shelf: in situ observations. *Journal of Geophysical Research: Oceans*, *121*(09): 6671-6695.

Pullen, J.; Allard, R.; Seo, H.; Miller, A. J.; Chen, S.; Pezzi, L. P.; Smith, T.; Chu, P.; Alves, J.; Caldeira, R. 2017. Coupled oceano-atmosphere forecasting at short and medium time scales. *Journal of Marine Research, 75*(06): 877-921.

Santos-Alamillos, F.J.; Pozo-Vásquez, D.; Ruiz-Arias, J.A.; Lara-Fanego, V. & Tovar-Pescador, J. 2013. Analysis of WRF Model Wind Estimate Sensitivity to Physics Parameterization Choice and Terrain Representation in Andalusia (southern Spain). *Journal of Applied Meteorology*, *52*: 1592-1609.

Seo, H.; Jochum, M.; Murtugudde, R. & Miller, A.J. 2006. Effect of ocean mesoscale variability on the mean state of tropical Atlantic climate. *Geophysical Research Letters, 33*: L09606.

Shchepetkin A.F. & McWilliams, J.C. 2003. A method for computing horizontal pressure-gradient force in an oceanic model with a nonaligned vertical coordinate. *Journal of Geophysical Research, 108*: 3090.

Shchepetkin A.F. & McWilliams, J.C. 2005. The Regional Ocean Modeling System: a split-explicit, free-surface, topography-following coordinates ocean model. *Ocean Modelling*, *9*: 347-404.

Shi, J.J.; Tao, W.K.; Matsui, T.; Cifelli, C.; Hou, A.; Lang, S.; Tokay, A.; Wang, N-Y.; Peters-Lidard, C.; Skofronick-Jacksona, G.; Rutledge, S. & Petersen, W. 2010. WRF simulations of the 20-22 January 2007 snow events of eastern Canada: Comparison with in situ and satellite observations. *Journal of Applied Meteorology and Climatology*, *49*: 2246-2266.

Skamarock, W.C.; Klemp, J.B.; Dudhia, J.; Gill, D.O.; Barker, D.M.; Wang, W. & Powers, J.G. 2008. *A Description of the Advanced Research WRF Version 3*. NCAR Technical Note. TN-475+STR. Boulder, 113 p.

Souza, R.B.; Mata, M.M.; Garcia, C.A.E.; Kampel, M.; Oliveira, E.N. & Lorenzzetti, J. 2006. Multi-sensor satellite and in situ measurements of a warm core eddy south if Brazil-Malvinas Confluence region. *Continental Shelf Research*, *24*: 241-262.

Souza, R.B. & Robinson, I.S. 2003. Lagrangian and satellite observations of the Brazilian Coastal Current. *Remote Sensing of Environment*, *100*: 52-66.

Stramma, L. & M. England. 1999. On the water masses and mean circulation of the South Atlantic Ocean. *Journal of Geophysical Research*, *104*(C9): 20863-20883.

Sverdrup, H.U.; Jhonson, M.W. & Fleming, R.H. 1942. *The Oceans: their Physics, Chemistry and General Biology*. New York, Prentice-Hall. 1087p.

Tao, W.K.; Shi, J.J.; Chen, S.S.; Lang, S.; Lin, P.L.; Hong, S.Y.; Peters-Ludard, C. & Hou, A. 2011. The impact of microphysical schemes on hurricane intensity and track. *Asia-Pacific Journal of Atmospheric Sciences*, *47*: 1-16.

Taylor, K.E. 2001. Summarizing multiple aspects of model performance in a single diagram. *Journal of Geophysical Research*, *106*: 7183-7192.

Taylor, P.K. & Yelland, M.J. 2001. The dependence of Sea Surface Roughness on the Height and Steepnes of the Waves. *Journal of Physical Oceanography*, *31*: 572-589.

Wajsowicz, R.C. 1993. A consistent formulation of the anisotropic stress tensor for use in models of the large-scale ocean circulation. *Journal of Computational Physics*, *105*: 333-338.

Warner, J.C.; Armstrong, B.; He, R. & Zambom, J.B. 2010. Development of a Coupled Ocean-Atmosphere-Wave-Sediment Transport (COAWST) Modeling System. *Ocean Modelling*, *35*: 230-244.

Warner, J.C.; Sherwood, C.R.; Signell, R.P.; Harris, C. & Arango, H.G. 2008. Development of a three-dimensional, regional, coupled wave, current, and sediment-transport model. *Computers and Geosciences*, *34*: 1284-1306.

Wilks, D.S. 1995. *Statistical Methods in the Atmospheric Sciences: An introduction*. Cambridge, Academic Press. 648 p.

Xie, S.P. 2004. Satellite observations of cool ocean–atmosphere interaction. *Bulletin of the American Meteorological Society*, *85*: 195-209.

Zhang, X.; Anagnostou, E.N.; Frediani, M.; Solomos, S. & Kallos, G. 2013. Using NWP simulations in Satellite Rainfall Estimation of Heavy Precipitation Events over Mountainous Areas. *Journal of Hydrometeorology*, *14*: 1844-1857.